Supporting information for

Fluorescent pattern discrimination towards metal ions by nanoparticles of bovine serum albumin as chemical nose/tongue

Yu-Lin Fan, Yi-Fan Lu, Xu-Yin Ding, Nai-Hong Wang, Feng Xu, Guoyue Shi, Min Zhang*

School of Chemistry and Molecular Engineering, Shanghai Key Laboratory for Urban Ecological Processes and Eco-Restoration, Engineering Research Centre for Nanophotonics and Advanced Instrument (Ministry of Education), East China Normal University, 500 Dongchuan Road, Shanghai 200241, China. Email: mzhang@chem.ecnu.edu.cn

1. Experimental Section

Chemicals and Materials. The following metal salts, $AgNO_3$, $AlCl_3$, $CaCl_2$, $CrCl_3$, $CuCl_2$, $CoCl_2$, $CdCl_2$, $FeCl_2$, $FeCl_3$, KCl, LiCl, $MgCl_2$, $MnCl_2$, $NiCl_2$, NaCl, $PbCl_2$, $ZnCl_2$, and other regents were reagent grade and ordered from Sinopharm Chemical Reagent Co. Ltd. (Shanghai, China). Bovine serum albumin (BSA), Ascorbic acid, Hemoglobin (from pig), Glycine, L-Cysteine, D-Leucine, L-Arginine and glutaraldehyde were purchased from Sigma−Aldrich (St. Louis, MO). Tris-HAc buffer (10 mM, pH 8.3) was prepared using metal free reagents in in Milli-Q water.

Apparatus and measurements. Dynamic Light Scattering (DLS) measurements were obtained by a Nano-ZS Zetzsozer ZEN3600 (Malvern Instruments Ltd., U.K.). Transmission electron microscope (TEM) image was recorded using a Transmission Electron Microscope (JEM-2100F, Japan) operated at 200 kV. Fluorescence spectroscopy was measured in a microplate reader (infinite M200 pro, TECAN, Switzerland) using a black 384-well microplate (Corning, U.S.A.) under 380 nm excitation. Fourier transform infrared spectroscopy (FTIR) spectra was obtained with a Nicolet optical bench (Nexus 670). And FTIR tested the freeze-dried $BSANs_{40}$ from 500 to 4000 nm.

$BSANS_n$ Preparation. 4 mL of ethanol solution was respectively and slowly added to 2 mL of BSA solution (5, 10, 20, 30 and 40 $mg \cdot mL^{-1}$) in the clean eggplant shaped bottle (25 ml) at room temperature under stir. Then the solutions became slightly opalescent. After mixing well, 16 μL of 50% (v/v) glutaraldehyde was added to these mixed suspensions above and the solutions became almost immediately milky. And we kept these suspensions stirring at room temperature for 18 h to induce cross-linking (Scheme 1a). The resulting $BSANs_n$ ($BSANs_5$, $BSANs_{10}$, $BSANs_{20}$, $BSANs_{30}$, and $BSANs_{40}$) were purified by centrifugation at 10000 rpm (10 min) and washing 3 times using Milli-Q water. Then we chose three of them as a sensor array ($BSANs_{10}$, $BSANs_{20}$ and $BSANs_{40}$). The three obtained $BSANs_n$ were constructed as a sensor array, and their solutions were diluted to 1.0 $mg \cdot mL^{-1}$, respectively. To keep them stable, we put them in fridge under 4℃.

Detection Procedures. The solutions of 18 kinds of metal ions at 50 μM were prepared. Then 10 μL $BSANs_n$ ($BSANs_{10}$, $BSANs_{20}$, and $BSANs_{40}$, all in 1.0 mg·mL^{-1}) solutions and 80 μL Tris-HAc buffer (10 mM, pH 8.5) were added. After incubating in the 384-well black microplate for 10 min at room temperature, the fluorescence intensity of $BSANs_n$ were recorded. The fluorescence change $(F_0-F)/F_0$ (F_0 and F are the fluorescence intensity at 526 nm in the absence and presence of metal ions) was used to evaluate the effect of various metal ions on the fluorescence of $BSANs_n$. Each metal ion was reacted with $BSANs_n$ sensor array in quintuplicate. The raw acquired data matrix (three $BSANs_n$ sensor array × eighteen metal ions × five replicates) was processed by principal component analysis (PCA, a statistical analysis method by SPSS). The heat map was obtained using GraphPad Prism 7.0 software based on the $(F_0-F)/F_0$ data, corresponding to the fluorescence patterns of $BSANs_n$ sensor array toward metal ions.

The single metal ion Cu^{2+} with concentration of 0.1, 0.5, 1, 5, 8, 10, 20, 30, 40, 50 μM, Ni^{2+} with concentration of 0.5, 1, 5, 10, 20, 30, 40, 50 μM, Fe^{3+} with concentration of 0.1, 1, 8, 10, 40, 50, 80, 100 μM, Co^{2+} with concentration of 1, 2, 5, 8, 10, 15, 20, 25, 30, 40, 45, 50 μM were prepared and Fe^{2+} with concentration of 0.5, 1, 5, 8, 10, 20, 30, 40, 50 μM were prepared. The detection procedure was same as above.

Binary mixtures of Fe^{3+}/Fe^{2+}, Cu^{2+}/Fe^{2+}, Cu^{2+}/Cr^{3+} were prepared respectively with mass ratio of 0/50, 10/40, 20/30, 25/25, 30/20, 40/10 and 50/0 (the total concentration was 50 μM). And binary mixtures of Cr^{3+}/Cr^{6+}, was prepared with mass ratio of 0/10, 2/8, 4/6, 5/5, 6/4, 8/2, 10/0 (the total concentration was 10 μM). The detection procedure was same as single metal ion.

The biofluids samples, including artificial urine, artificial saliva, artificial human sweat and human urine, were spiked with the mixed metal ions above respectively and tested against the three kinds of $BSANs_n$ sensors five times to give a 4 targets × 3 arrays × 5 replicates data matrix. The experimental procedure was same as above.

2. Supplementary Figures

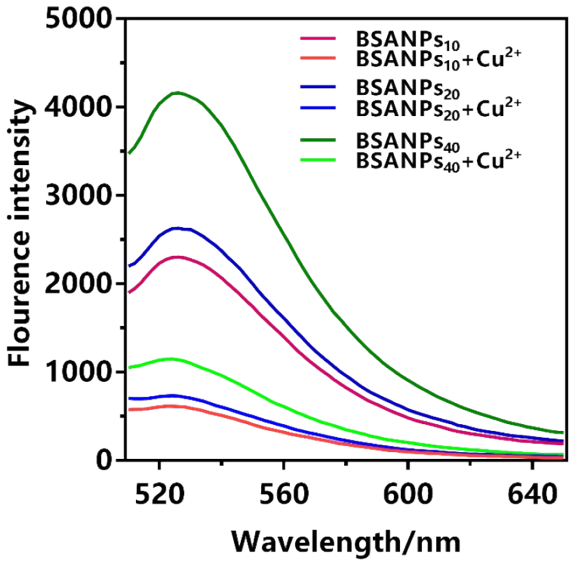

Figure S1. Fluorescence spectra of different $BSANs_n$ sensors in the absence or present of 50 μM Cu^{2+}.

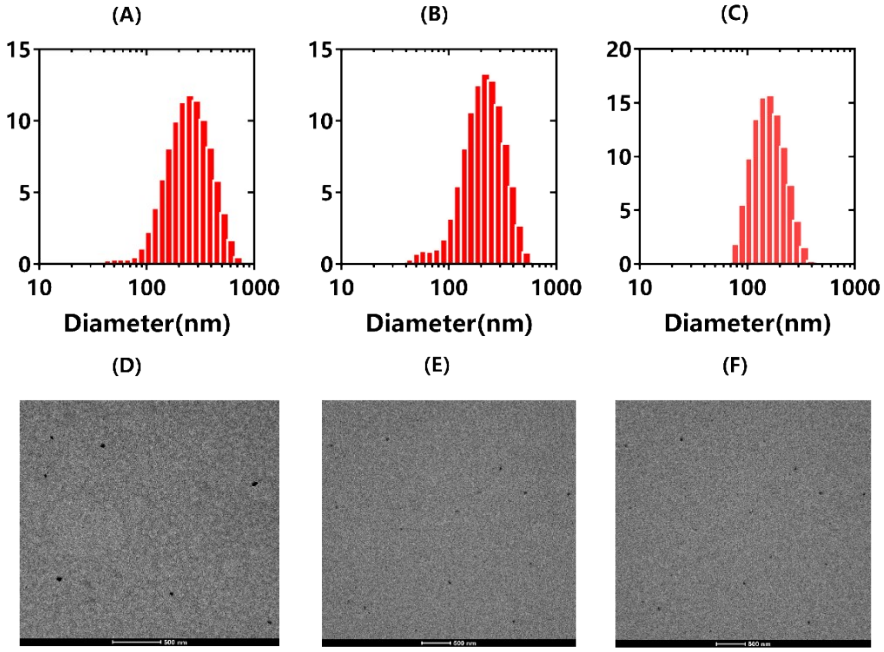

Figure S2. DLS measurement of the hydrodynamic diameters of (A) $BSANs_{10}$: 50±5nm, (B) $BSANs_{20}$: 30±5nm, and (C) $BSANs_{40}$: 20±5nm, respectively. TEM images of (D) $BSANs_{10}$ and (E) $BSANs_{20}$ (F) $BSANs_{40}$.

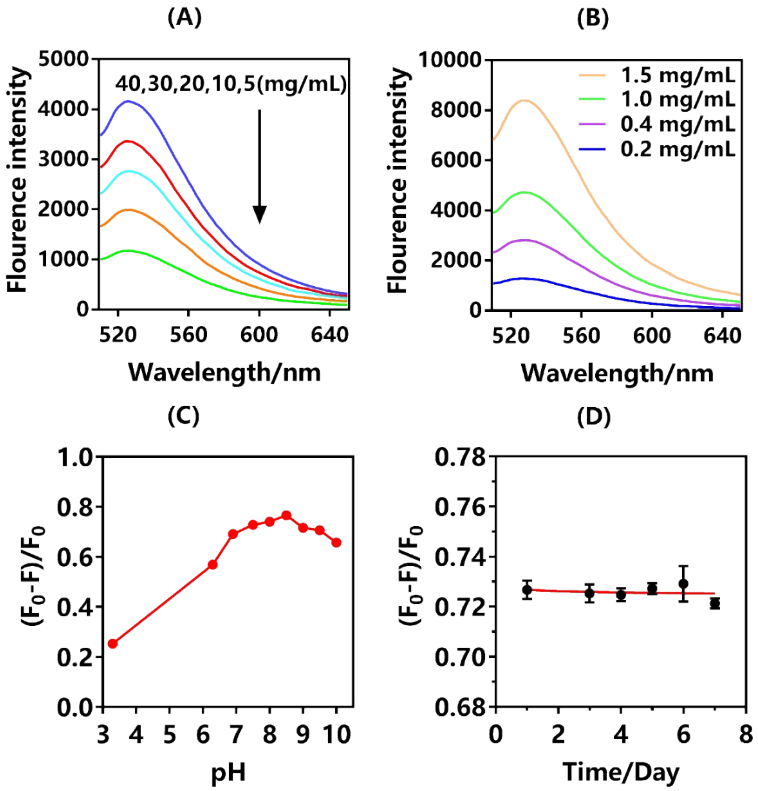

Figure S3. (A) The fluorescence intensity of different $BSANs_n$ sensors made by different concentrations of BSA (5, 10, 20, 30, 40 mg·mL^{-1}). (B) The fluorescence intensity of $BSANs_{40}$ sensor

with different concentrations (1.5, 1.0, 0.4, 0.2 mg·mL^{-1}). (C) The fluorescence quenching rate of $BSANs_{40}$ sensor toward Cu^{2+} (50 μM) under varying pH (3.3, 6.3, 6.9, 7.5, 8, 8.5, 9.5, 10). (D) The Fluorescence quenching rate of $BSANs_{40}$ sensor toward Cu^{2+} (50 μM) under pH 8.5 in a week.

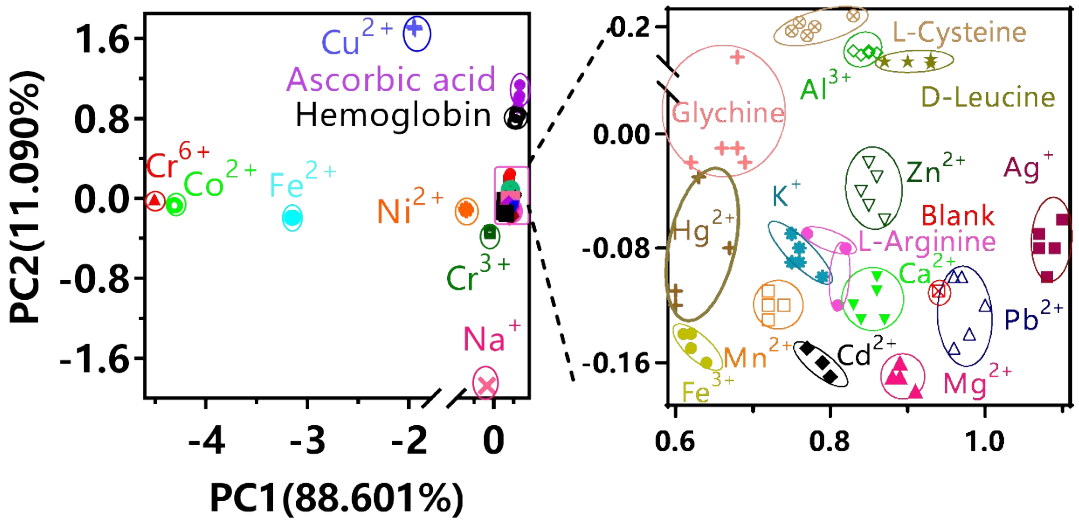

Figure S4. PCA scatter graph of 18 metal ions and 6 biological samples (Ascorbic acid, Hemoglobin, Glycine, L-Cysteine, D-Leucine, L-Arginine) generated by the $BSANs_n$ sensing system (3 sensors × 24 samples × 5 trials, the concentration of all samples is 50 μM).

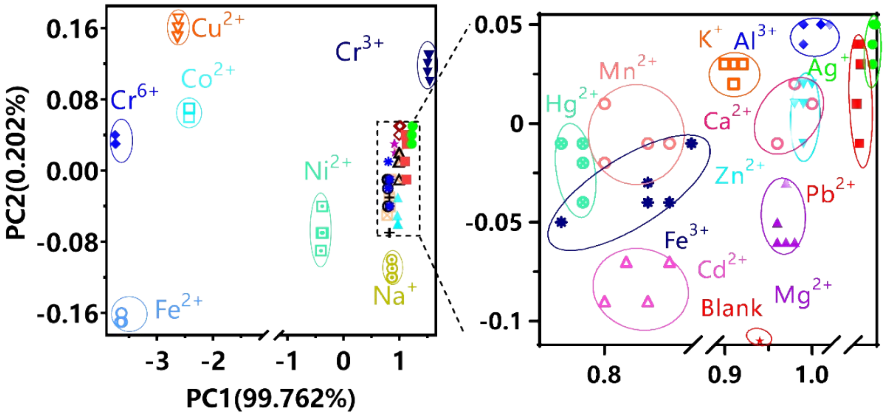

Figure S5. PCA scatter graph of 18 metal ions generated by the $BSANs_n$ ($BSANs_{10}$, $BSANs_{20}$, $BSANs_{40}$) sensing system (3 sensors × 24 samples × 5 trials, the concentration of all samples is 50 μM).

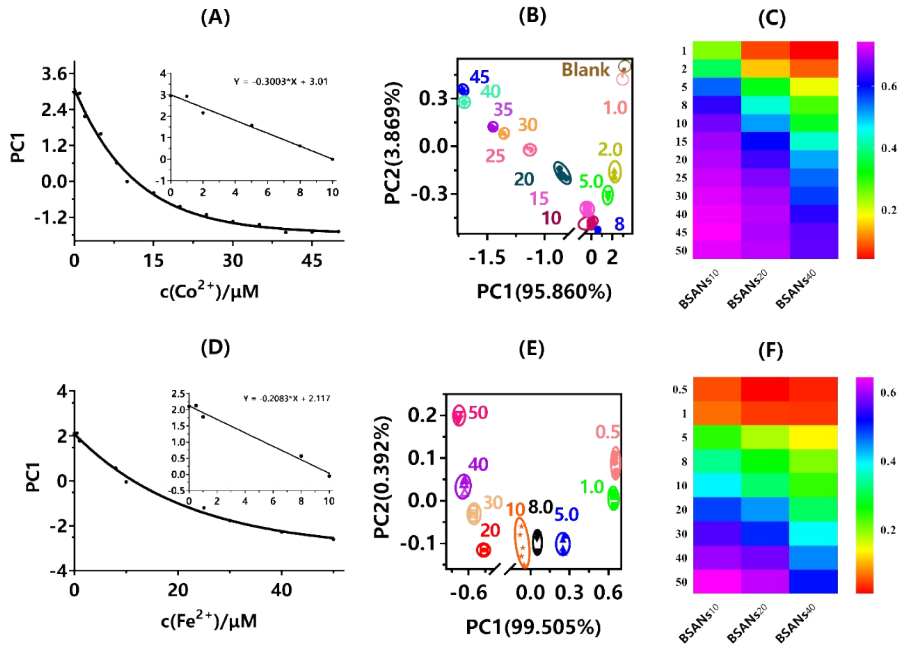

Figure S6. Discrimination of various concentrations of metal ions using $BSANs_n$ sensor array. Plots of PC1 vs the concentrations of (A) Co^{2+}, inset equation: Y = -0.3003*X + 3.001; (D) Fe^{2+}, inset equation: Y = -0.2083*X + 2.117; Canonical score plots and heat map for fluorescence response patterns obtained with $BSANs_n$ sensors against varying concentrations of (B, C) Co^{2+} (1, 2, 5, 8, 10, 20, 25, 30, 40, 45, 50 μM) and (E, F) Fe^{2+} (0.5, 1, 5, 8, 10, 20, 30, 40, 50 μM).

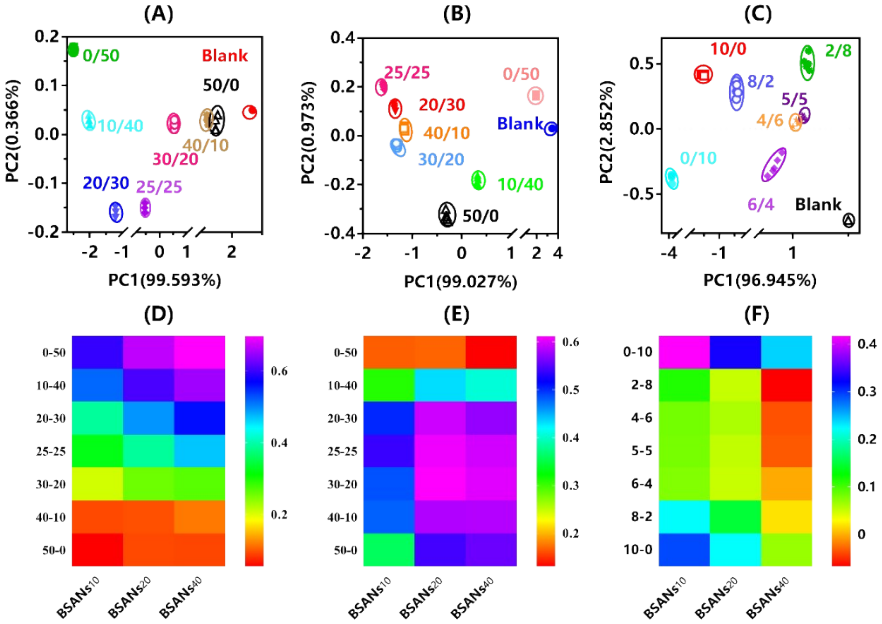

Figure S7. (A, B, C) Canonical score plot for fluorescence response patterns of $BSANs_n$ sensors against the mixture of Fe^{2+}/Fe^{3+} (0/50, 10/40, 20/30, 25/25, 30/20, 40/10, 50/0), Cu^{2+}/Cr^{3+} (0/50, 10/40, 20/30, 25/25, 30/20, 40/10, 50/0), Cr^{3+}/Cr^{6+} (0/10, 2/8, 4/6, 5/5, 6/4, 8/2, 10/0) in buffer. (D, E, F) Heat map derived from the fluorescence response patterns of $BSANs_n$ sensor array against the mixture of Cu^{2+}/Cr^{3+}, Cr^{3+}/Cr^{6+}, Fe^{2+}/Fe^{3+} in buffer.

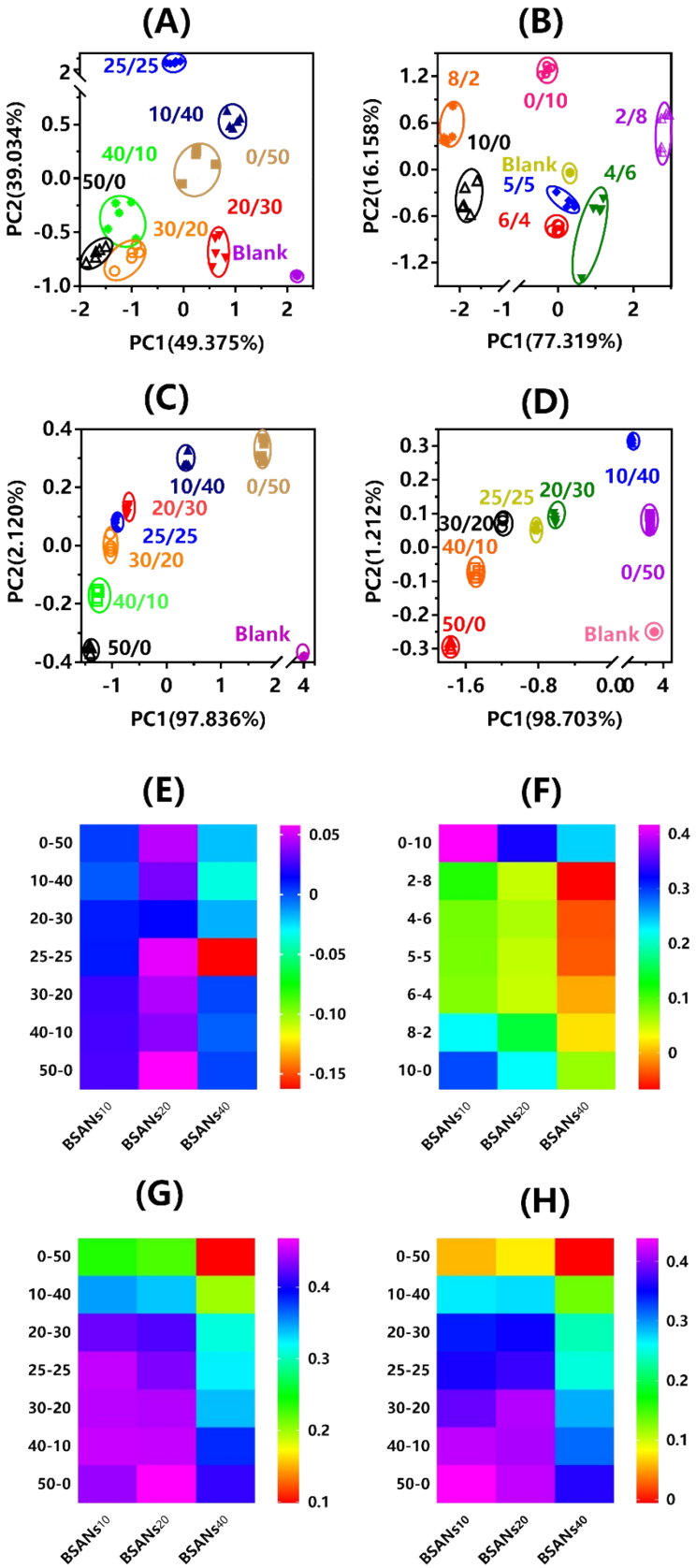

Figure S8. (A, B, C, D) Canonical score plots for fluorescence response patterns of $BSANs_n$ sensors

against the mixture of Fe^{2+}/Fe^{3+} (0/50, 10/40, 20/30, 25/25, 30/20, 40/10, 50/0) in artificial saliva, Cr^{3+}/Cr^{6+} (0/10, 2/8, 4/6, 5/5, 6/4, 8/2, 10/0) in artificial urine, Cu^{2+}/Cr^{3+} (0/50, 10/40, 20/30, 25/25, 30/20, 40/10, 50/0) in artificial urine and Cu^{2+}/Fe^{3+} (0/50, 10/40, 20/30, 25/25, 30/20, 40/10, 50/0) in artificial sweat.

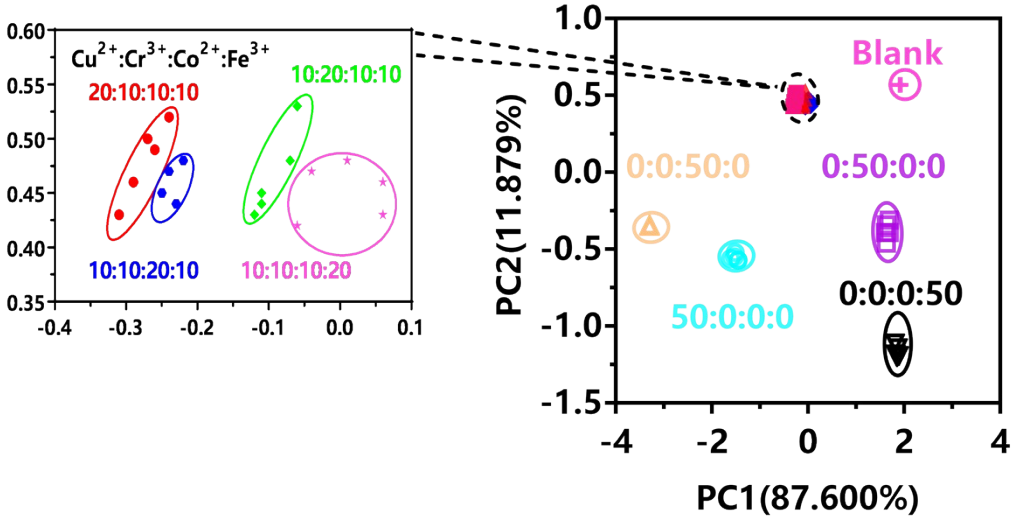

Figure S9. Canonical score plots for fluorescence response patterns of $BSANs_n$ sensors against the mixture of Cu^{2+}: Cr^{3+}: Co^{2+}: Fe^{3+} (50:0:0:0, 0:50:0:0, 0:0:50:0, 0:0:0:50, 20:10:10:10, 10:20:10:10, 10:10:20:10, 10:10:10:20) in artificial urine.

Table S1. An overview on recently reported sensor array for differentiating of metal ions

Sensor array	Sensors	Targets	Analytical range (μM)		Detection of Limit (μM)	References
BSANPs	3	18	Cu^{2+}	0.1-10	0.025	This work
			Ni^{2+}	0.1-10	0.083	
			Co^{2+}	0.1-10	0.080	
			Fe^{2+}	0.1-10	0.115	
Triazole-carboxyl Ag NPs	3	16	Cu^{2+}	0.1-6	0.07-0.21	[1]
			Ni^{2+}	0.1-12	0.48	
			Co^{2+}	0.1-12	0.22	
			Fe^{2+}	0.1-12	0.51	
NRFSA	3	15	Cu^{2+}	20-80	/	[2]
			Fe^{2+}	10-100	/	
GOx_e-based assay	3	12	Cu^{2+}	20-90	20	[3]
			Co^{2+}	25-200	25	

Table S2. Detection of Cu^{2+} and Co^{2+} in Urine Using $BSANs_n$ Sensor Array

Entry	Metal ion	Actual (μM)	ICP-AES (μM)	BSANs (μM)	Recovery	RSD
Urine	Cu^{2+}	5	5.00	4.93	98.6%	1.17%
		25	25.32	24.8	99.2%	1.02%
	Co^{2+}	5	5.06	6	120%	1.60%
		8	7.98	7.97	99.6%	2.14%

Table S3. Detection of Co^{2+} in Artificial Biofluids Using $BSANs_n$ Sensor Array

Entry	Actual (μM)	ICP-AES (μM)	BSANs (μM)	Recovery	RSD
Urine	2.5	2.64	2.37	95%	0.64%
	5	5.06	4.77	95%	0.64%
Sweat	2.5	2.5 6	2.47	99%	0.43%
	8	7.99	8.17	102%	5.23%

3. References

1 Y. Liu, M. Mettry, A. D. Gill, L. Perez, W. Zhong and R. J. Hooley, Analytical Chemistry., 2017, 89, 11113-111121.

2 S. A. Moayed, H. Golmohammadi and M. R. H. Nezhad, Nanoscale., 2018, 10, 2492-2502.

3 C. Chen, Q. Xie, L. Wang, C. Qin, F. Xie, S. Yao and J. Chen, Analytical Chemistry., 2011, 83, 2660-2666.